

# Nonreciprocal $\mathcal{PT}$ -symmetric phase transition in a non-Hermitian chiral quantum optical system

Miao Cai,<sup>1,\*</sup> Jiang-Shan Tang,<sup>1,2,\*</sup> Ming-Yuan Chen,<sup>1</sup> and Keyu Xia<sup>1,2,†</sup>

<sup>1</sup>College of Engineering and Applied Sciences, National Laboratory of Solid State Microstructures, and Collaborative Innovation Center of Advanced Microstructures, Nanjing University, Nanjing 210023, China

<sup>2</sup>Hefei National Laboratory, Hefei 230088, China

(Dated: April 22, 2024)

Phase transitions, non-Hermiticity and nonreciprocity play central roles in fundamental physics. However, the triple interplay of these three fields is of lack in the quantum domain. Here, we show nonreciprocal parity-time-symmetric phase transition in a non-Hermitian chiral quantum electrodynamical system, caused by the directional system dissipation. In remarkable contrast to previously reported nonreciprocal phase transitions, the nonreciprocal parity-time-symmetric phases appear even when the atom-resonator coupling is reciprocal. Nonreciprocal photon blockade is obtained in the nonreciprocal phase region. These results may deepen the fundamental insight of nonreciprocal and non-Hermitian quantum physics, and also open a new door for unconventional quantum manipulation.

**Introduction.**—Phase transitions, characterized by continuous change of system properties driven by external parameters, are crucially important to fundamental physics. Phenomena related to phase transitions range from our daily-life experience of ice melting to far more exotic superfluid Mott-insulator phase transitions [1], from microscopic quark-level matter transitions [2] to cosmological phase transitions in the early Universe [3], and from single-particle [4] to many-body Dicke quantum phase transitions [5]. The investigation on zero-temperature phase transitions, for the first time, reveals the role of quantum effects in phase transitions, opening up the field of quantum phase transition [6–9]. Quantum phase transitions are vital for understanding the evolution of matter phases [10–12] and have been widely observed or predicted in various systems ranging from condensed-matter systems [13] and atomic systems [1] to optical systems [14–16].

A non-Hermitian system displays a transition between the unbroken and broken parity-time ( $\mathcal{PT}$ )-symmetric phases at its exceptional point [17]. A variety of exotic physics have been revealed in a non-Hermitian system associated with the  $\mathcal{PT}$ -symmetric phase transitions [18–24]. The  $\mathcal{PT}$ -symmetric phase transition of a quantum spin has also been reported [25–28]. Now the non-Hermitian system emerges as a highly appealing platform for studying phase transitions in both the classical and quantum domains.

Nonreciprocity is a concept equally important to phase transition and non-Hermiticity. It plays an indispensable role in useful applications such as optical isolation [29–45] and sensing enhancement [46–54]. Nonreciprocity shows parallel importance in fundamental physics. Nonreciprocal interaction between different parties of a system, as a vital mechanism to build a non-Hermitian system, has been explored to study one-way topological solitons in active matter [55], novel phase transitions [56–63], the skin effect [64, 65], band structure in a Floquet medium [66] and even to distinction of fundamental quantum effects [67]. By breaking the time-reversal ( $\mathcal{T}$ ) symmetry via nonreciprocal modulation, a non-Hermitian

Aharonov-Bohm effect and phase transitions with unconventional phononic  $\mathcal{PT}$  symmetry are observed in an optomechanical resonator [24]. Despite great advances, nonreciprocal phase transitions in a non-Hermitian quantum system remains unexplored so far in the case without intermode nonreciprocal interaction or control.

In this work, by leveraging chiral dissipation induced by breaking the  $\mathcal{T}$  symmetry of a non-Hermitian cavity quantum electrodynamical system (cQED), we show nonreciprocal  $\mathcal{PT}$ -symmetric phase transitions *without the need of nonreciprocal interaction or modulation*. In combination with a chiral atom-resonator coupling, we attain reciprocal photon transmission but strong nonreciprocal quantum correlation, implying nonreciprocal photon blockade.

**System and model.**—The non-Hermitian chiral cQED system is schematically shown in Fig. 1(a). It consists of a V-type atom coupling to a microring resonator. To probe the system dynamics, a single-mode optical waveguide is coupled to the resonator. This waveguide causes the fields in the resonator to decay with rate  $\kappa_{\text{ex}}$ .

The resonator supports two whispering-gallery modes (WGMs) propagating in the counterclockwise (CCW) and clockwise (CW) directions, respectively. We dub the system dynamics associated with the CCW and CW modes as the forward and backward cases. These CW and CCW modes are degenerate in resonance frequency, denoted as  $\omega_r$ , and intrinsically decay with rate  $\kappa_{\text{in}}$ , yielding the same overall decay rate  $\kappa = \kappa_{\text{in}} + \kappa_{\text{ex}}$ . Noticeably, the evanescent fields of their quantum vacuum fluctuation can be circularly polarized near the resonator surface. Their polarizations are directional under time reversal and thus chiral [68]. According to numerical simulations [69] and theoretical analysis [70], the evanescent field of the CCW (CW) mode is left-hand (right-hand) circularly polarized, denoted as  $\sigma_+$  ( $\sigma_-$ ).

The quantum vacuum field of the resonator mode can strongly interact with an atom nearby the resonator surface. We consider a V-type atom coupling to the resonator. The ground and two excited states of the atom are  $|0\rangle, |1\rangle, |2\rangle$ . The CCW and CW modes couples to the transitions  $|0\rangle \leftrightarrow |1\rangle$  and  $|0\rangle \leftrightarrow |2\rangle$ , with strengths  $g_{\text{CCW}}$  and  $g_{\text{CW}}$ , respectively. The states  $|1\rangle$  and  $|2\rangle$  decay with rates  $\gamma_{\text{CCW}}$  and  $\gamma_{\text{CW}}$ . We consider the case of  $\gamma_{\text{CCW}} > \gamma_{\text{CW}}$ ,  $\kappa \neq \gamma_{\text{CW}}$  and

\* These two authors contributed equally

† keyu.xia@nju.edu.cn

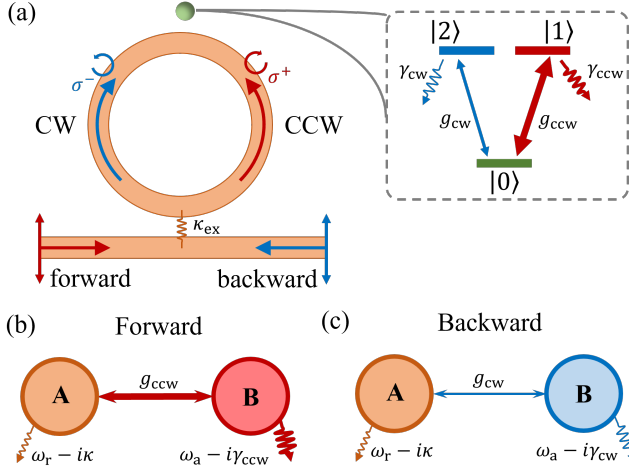


FIG. 1. (a) Schematic for nonreciprocal  $\mathcal{PT}$ -symmetric phase transition in a non-Hermitian chiral cQED system. The CCW (CW) mode couples to the V-type atom via its  $\sigma_+$ -polarized ( $\sigma_-$ -polarized) evanescent field and drives the atomic transition  $|0\rangle \leftrightarrow |1\rangle$  ( $|0\rangle \leftrightarrow |2\rangle$ ) with strength  $g_{CCW}$  ( $g_{CW}$ ). The states  $|1\rangle$  and  $|2\rangle$  respectively decay with rates  $\gamma_{CCW}$  and  $\gamma_{CW}$ . An optical waveguide is used to probe the nonreciprocal behaviors of the system with the forward and backward inputs. The CW and CCW modes decay with rate  $\kappa_{in}$  intrinsically and with rate  $\kappa_{ex}$  externally to the waveguide. (b) and (c) Single-excitation non-Hermitian model for the forward and backward cases.

$\kappa \neq \gamma_{CCW}$ , leading to non-Hermiticity in both the forward and backward cases. The system Hamiltonian including the atom-resonator interaction is given by  $H_s/\hbar = \omega_a(\sigma_{20}\sigma_{02} + \sigma_{10}\sigma_{01}) + \omega_r(a_{CW}^\dagger a_{CW} + a_{CCW}^\dagger a_{CCW}) + g_{CW}(a_{CW}^\dagger \sigma_{02} + \sigma_{20} a_{CW}) + g_{CCW}(a_{CCW}^\dagger \sigma_{01} + \sigma_{10} a_{CCW})$ , where the atomic operators are defined as  $\sigma_{fi} = |f\rangle\langle i|$ ,  $a_{CW}$  and  $a_{CCW}$  are the annihilation operators of the CW and the CCW mode, respectively,  $\hbar$  is the Planck constant. To probe the nonreciprocal behavior of the system, we input weak fields  $\alpha_{in}$  and  $\beta_{in}$  with frequency  $\omega_p$  in the forward and backward cases, respectively. The Hamiltonian describing this probe takes the form  $H_D/\hbar = i\sqrt{2\kappa_{ex}}\alpha_{in}a_{CW}^\dagger + i\sqrt{2\kappa_{ex}}\beta_{in}a_{CCW}^\dagger + H.c.$  with  $|\alpha_{in}|^2$  and  $|\beta_{in}|^2$  representing the input photon fluxes. Then, the system dynamics is determined by the quantum master equation,

$$\dot{\rho} = -i[H/\hbar, \rho] + \mathcal{L}\{\kappa, a_{CW}, \rho\} + \mathcal{L}\{\kappa, a_{CCW}, \rho\} + \mathcal{L}\{\gamma_{CW}, \sigma_{02}, \rho\} + \mathcal{L}\{\gamma_{CCW}, \sigma_{01}, \rho\}, \quad (1)$$

where  $H = H_s + H_D$ ,  $\rho$  is the system density matrix,  $\mathcal{L}$  is the Lindblad superoperator describing the system dissipation and defined as  $\mathcal{L}\{\xi, o, \rho\} = \xi(2o\rho o^\dagger - o^\dagger o\rho - \rho o^\dagger o)$  with  $\xi \in \{\kappa, \gamma_{CCW}, \gamma_{CW}\}$  and  $o \in \{a_{CW}, a_{CCW}, \sigma_{02}, \sigma_{01}\}$ . Note that the CCW and CW modes are orthogonal in polarization and drives the two atomic transitions separately. Thus, the system exhibits chiral atomic dissipation under time reversal. To characterizing the transmission and full-quantum dynamics of the system, we numerically solve the master equation and truncate the resonator mode to the fourth photonic Fock state.

The key point of this work is that the cQED system is non-Hermitian and possesses quantum chirality, induced by breaking the  $\mathcal{T}$  symmetry. Below, we show these properties and the

system eigenfrequencies in the single-excitation space. Under weak-input condition, the system reduces to two decoupled cQED subsystems. Each includes a resonator mode and a two-level atom but with different dissipation rates, thus is non-Hermitian. Particularly, in the single-excitation space, these non-Hermitian subsystems can be modeled as two-mode systems consisting of a cavity mode A (orange circle) coupling to a cavity mode B (red or blue circle) with strength  $g_{CCW}$  and  $g_{CW}$ , as shown in Figs. 1(b) and (c). The mode A maintains the loss rate of  $\kappa$ , whereas the mode B decays with rate  $\gamma_{CCW}$  and  $\gamma_{CW}$  in the forward and backward cases, respectively. Thus, the  $\mathcal{T}$  symmetry breaks and we “see” two different non-Hermitian subsystems in opposite directions. The Hamiltonians for the two models including the mode dissipation can be written as [71],

$$H_x = \begin{pmatrix} \omega_r - i\kappa & g_x \\ g_x & \omega_a - i\gamma_x \end{pmatrix}, \quad (2)$$

with  $x = \text{“CW”}$  and  $x = \text{“CCW”}$  representing the forward and backward cases, respectively. Obviously,  $H_{CCW} \neq H_{CW}$  when  $\gamma_{CCW} \neq \gamma_{CW}$  or  $g_{CCW} \neq g_{CW}$  or both. The eigenvalues of this Hamiltonian are  $E_{\pm, x} = (\omega_+ - i\gamma_{+, x}) \pm \sqrt{(\omega_- - i\gamma_{-, x})^2 + g_x^2}$ , where  $\omega_{\pm} = (\omega_r \pm \omega_a)/2$  and  $\gamma_{\pm, x} = |\kappa \pm \gamma_x|/2$ . Under the atom-resonator resonance condition that  $\omega_a = \omega_r = \omega_0$ , yielding  $\omega_- = 0$  and  $\omega_+ = \omega_0$ , the eigenvalues become

$$E_{\pm, x} = (\omega_0 - i\gamma_{+, x}) \pm \sqrt{g_x^2 - \gamma_{-, x}^2}. \quad (3)$$

Both the eigenvectors and eigenvalues coalesce at the so-called exception point (EP)  $g_{EP, x} = \gamma_{-, x}$ , associated with the  $\mathcal{PT}$ -symmetric phase transition. Because  $g_{EP, CW} \neq g_{EP, CCW}$ , phase transitions can occur at different coupling strength in the forward and backward cases. Thus, the original cQED system can display nonreciprocal  $\mathcal{PT}$ -symmetric phase transitions in the quantum domain when  $g_{EP, CW} < g_{CW} < g_{EP, CCW} < g_{CCW}$  as the atom-surface distance  $r$  varies. We define the detuning between the input probe field and the atom-resonator system as  $\Delta_p = \omega_0 - \omega_p$ .

A rubidium or cesium (Cs) atom nearby a bottle-shaped or integrated microring resonator can be used to realize our chiral cQED system [33–35, 69]. Throughout our investigation below, we consider a Cs atom resonantly coupling to the resonator via the evanescent quantum vacuum fields of the CW and CCW modes such that  $\omega_- = 0$ . The Cs atom is prepared in the ground state  $|6^2S_{1/2}, F=4, m_F=4\rangle$ . The excited states are  $|1\rangle = |6^2P_{3/2}, F'=5, m_F'=5\rangle$  and  $|2\rangle = |6^2P_{3/2}, F'=5, m_F'=3\rangle$ . The atom couples to the  $\sigma_+$  and  $\sigma_-$  field with different dipole moments  $d_+$  and  $d_-$  that  $d_+ = \sqrt{45}d_-$  [72]. Thus, we have  $g_{CW} = g_{CCW}/\sqrt{45}$  and  $\gamma_{CW} = \gamma_{CCW}/45$ . Note that the coupling strength exponentially increases as the distance  $r$  between the atom and the resonator surface decreases. This allows us to tune the atom-resonator coupling and dynamically study the  $\mathcal{PT}$ -symmetric phase transition of the system. For simplicity, we choose the following normalized system parameters for our model and numerical simulations:  $\gamma_{CW} = 1, \gamma_{CCW} = 45, \kappa_{in} = 0.5, \kappa_{ex} = 2.5$  that  $\gamma_{CW} < \kappa_{ex} < \gamma_{CCW}$ , yielding  $g_{EP, CCW} = 21$  and  $g_{EP, CW} = 1$ .

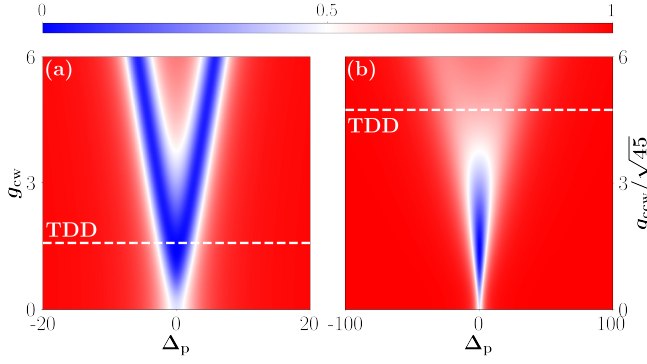


FIG. 2. Resonator transmission with respect to the atom-resonator coupling strength and the frequency detuning under (a) the CW mode and (b) the CCW mode excitation. The white dashed lines labeled with “TDD” indicate the critical coupling strengths where transmission dip degeneration happens.

*Nonreciprocal transmission.*—For the purpose of experimental test, we use the system transmission to characterize the nonreciprocal  $\mathcal{PT}$ -symmetric phase transition in our chiral cQED system. To do so, we firstly investigate the nonreciprocal resonator transmission in the two cases. The resonator transmission versus the atom-resonator coupling strength and the probe detuning are presented in Fig. 2. In comparison of the transmissions, the relation  $g_{\text{CW}} = g_{\text{CCW}}/\sqrt{45}$  maintains. Thus, the CCW coupling strength is scaled as  $g_{\text{CCW}}/\sqrt{45}$  in Fig. 2. The transmission spectra gradually change from singlet-dip to doublet-dip profiles as the coupling strength increases in both cases. By setting the derivative of the transmission zero [73], we obtain the points of transmission dip degeneracy (TDD), corresponding to a critical coupling strength

$$g_{\text{TDD},x} = \sqrt{\left(-\xi_{\text{TDD},x} + \sqrt{\xi_{\text{TDD},x}^2 - 4\zeta_{\text{TDD},x}\eta_{\text{TDD},x}}\right)/2\zeta_{\text{TDD},x}}, \quad (4)$$

where  $x \in \{\text{CW}, \text{CCW}\}$ ,  $\zeta_{\text{TDD},x} = 2\gamma_x + \kappa_{\text{in}}$ ,  $\xi_{\text{TDD},x} = 2\gamma_x^2\kappa_{\text{in}} - \gamma_x^3 - \gamma_x\kappa_{\text{ex}}^2 + \gamma_x\kappa_{\text{in}}^2$  and  $\eta_{\text{TDD},x} = -\kappa_{\text{in}}\gamma_x^4$ . When the coupling exceeds these critical values, the transmission spectral splittings occur. Note that a non-Hermitian sensor exhibits unprecedented enhancement of sensitivity around the transmission peak degeneracy [74]. The TDD may have the potential in sensing enhancement.

By substituting system parameters into Eq. 4, we obtain  $g_{\text{TDD,CW}} = 1.58$  and  $g_{\text{TDD,CCW}} = 31.78 \approx 4.74\sqrt{45}$  in the CW and CCW case, respectively. The critical coupling strengths are marked with white dashed lines in Fig. 2. In our proposed system, as the atom-surface distance decreases, both coupling strengths  $g_{\text{CW}}$  and  $g_{\text{CCW}}$  increase. Thus,  $g_{\text{TDD,CW}} \neq g_{\text{TDD,CCW}}/\sqrt{45}$  implies the different critical atom-surface distance in two cases where the transmission spectrum splits. These resonator transmissions under weak excitation provide an experimentally accessible way to extract the system eigenfrequency in the single-excitation space.

*Nonreciprocal phase transition.*—Below we characterize the nonreciprocal  $\mathcal{PT}$ -symmetric phase transition with the resonator transmission. In our system, the eigenfrequencies

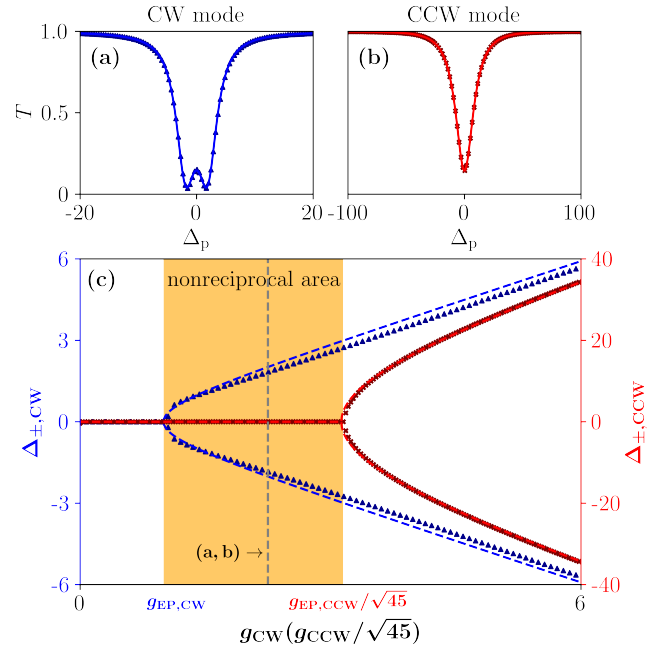


FIG. 3. (a) Transmissions at  $g_{\text{CW}} = 2.25$  in the forward case. (b) Transmissions at  $g_{\text{CCW}} = \sqrt{45}g_{\text{CW}} = 15.09$  in the backward case. In (a) and (b), solid curves are results of numerical simulation. Dots represent fitting using Eq. 5. (c) Eigenfrequencies with respect to  $\omega_p$  in the forward (red markers and curves) and backward (blue markers and curves) cases. The markers are numerical results. The dashed curves are fittings.

can be extracted from the resonator transmission spectrum by fitting it with the following function [75],

$$T(\Delta_p) \sim \frac{1 - c_1 \frac{\Gamma_{+,x}\Gamma_{-,x}}{[(\Delta_p - \Delta_{+,x})^2 + \Gamma_{+,x}^2][(\Delta_p - \Delta_{-,x})^2 + \Gamma_{-,x}^2]} - c_2 \frac{\Gamma_{+,x}^2\Gamma_{-,x}^2}{[(\Delta_p - \Delta_{+,x})^2 + \Gamma_{+,x}^2]^2[(\Delta_p - \Delta_{-,x})^2 + \Gamma_{-,x}^2]^2}}{x \in \{\text{CW}, \text{CCW}\}}, \quad (5)$$

where  $\Delta_{\pm,x} = \text{Re}(E_{\pm,x}) - \omega_0$  are the detunings between the eigenmodes and the probe field,  $\Gamma_{\pm,x} = \text{Im}(E_{\pm,x})$ ,  $c_1$  and  $c_2$  are the fitting parameters. The second term represents the Lorentzian transmission spectrum away from the EP, while the third term is the squared-Lorentzian contribution near the EP [75]. The difference between the two eigenfrequencies can be extracted from fitting as  $\Delta E_x = \text{Re}(E_{+,x}) - \text{Re}(E_{-,x}) = \Delta_{+,x} - \Delta_{-,x}$ . A eigenfrequency splitting manifests the  $\mathcal{PT}$ -symmetric phase transition [17].

Figures 3(a) and (b) show the numerical results and fittings of the transmission spectra at  $g_{\text{CCW}} = 15.09$  and  $g_{\text{CW}} = 2.25$  in the forward and backward cases, respectively, indicated by the dashed vertical line in Fig. 3(c). The fittings with Eq. 5 are in excellent agreement with simulation results. The backward transmission splits and gives  $\Delta_{+, \text{CW}} - \Delta_{-, \text{CW}} = 1.84$ , close to the theoretical value 2.02 according to the single-

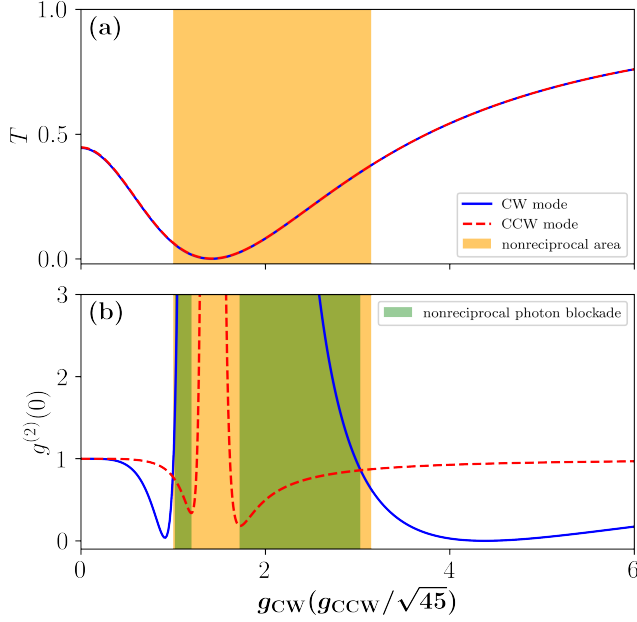


FIG. 4. (a) The resonator transmission with  $\Delta = 0$  with respect to the atom-resonator coupling strength under the CW (blue line) and the CCW (red dashed line) mode excitations. Orange shaded area represents nonreciprocal  $\mathcal{PT}$ -symmetric phase transition area. (b) The second-order quantum correlation values of the system versus the coupling strength under the CW and the CCW mode excitations. Green shaded area represents nonreciprocal photon blockade.

excitation model Eq. 3. It means the backward subsystem is in the unbroken  $\mathcal{PT}$ -symmetric phase. In contrast, we obtain  $\Delta_{+,CCW} - \Delta_{-,CCW} = 0$  in the forward case. Thus, the eigenfrequencies are degenerate, manifesting the broken  $\mathcal{PT}$  symmetry.

The eigenfrequencies can be extracted with high precision from the transmission spectra with Eq. 5. Figure 3(c) displays the eigenfrequencies as a function of the coupling strengths in the forward and backward cases. The numerical values are in good coincidence with the single-excitation model. Phase transitions occurs at EPs. Interestingly, the cQED system shows nonreciprocal  $\mathcal{PT}$ -symmetric phase transition as the atom-resonator interaction increases. When the interaction is weak that  $g_{CW} < g_{EP,CW}$ , the system is in the broken  $\mathcal{PT}$ -symmetric phase for the CW and CCW cases. The symmetry maintains in both cases when the interaction increases to strong enough that  $g_{CCW} > g_{EP,CCW}$ . Remarkably, the system exhibits nonreciprocal  $\mathcal{PT}$ -symmetric phase transitions at  $g_{EP,CW}$  and  $g_{EP,CCW}$ . At  $g_{EP,CW}$ , phase transition happens in the backward subsystem, but the  $\mathcal{PT}$  symmetry remains in the forward one. As the atom-resonator coupling increases to  $g_{EP,CCW}$ , the forward subsystem displays the  $\mathcal{PT}$ -symmetric phase transition. In the middle of

$g_{EP,CW} < g_{CW}(g_{CCW}/\sqrt{45}) < g_{EP,CCW}/\sqrt{45}$ , the forward and backward subsystems lie in essentially different phases.

**Nonreciprocal photon blockade.**—Nonreciprocal  $\mathcal{PT}$ -symmetric phase transitions are available when the coupling or the dissipation are different in the forward and backward cases. By combining the chiral coupling and dissipation, our system presents nonreciprocal photon blockade in the nonreciprocal phase region. As shown in Fig. 4(a), the resonant transmission ( $\Delta_p = 0$ ) are equal for opposite inputs as the coupling strengths varies. In the classical angle, the system is reciprocal. In Fig. 4(b), we study the quantum correlation properties of the system through numerical simulations. We calculate the equal-time second-order correlation function  $g_x^{(2)}(0) = \langle a_{out,x}^\dagger a_{out,x}^\dagger a_{out,x} a_{out,x} \rangle / \langle a_{out,x}^\dagger a_{out,x} \rangle^2$  with  $x \in \{CW, CCW\}$ , where  $a_{out,CW} = \alpha_{in} - \sqrt{2\kappa_{ex}}a_{CW}$  and  $a_{out,CCW} = \beta_{in} - \sqrt{2\kappa_{ex}}a_{CCW}$  [76]. We obtain two coupling regions allowing nonreciprocal photon blockade. When  $1.02 < g_{CW} < 1.20$  or  $1.72 < g_{CW} < 3.03$ , photon blockade is attained in the forward case, manifesting by  $g_{CCW}^{(2)}(0) < 1$ . In contrast, the backward subsystem shows strong photon bunching, indicated by  $g_{CW}^{(2)}(0) > 1$ . Thus, our system can achieve nonreciprocal photon blockade. It exhibits a pure nonreciprocal quantum behavior within the nonreciprocal quantum phase transition region.

**Conclusion and discussion.**—We have theoretically proposed a non-Hermitian cQED system for achieving nonreciprocal quantum phase transition. The underlying mechanism is either the chiral coupling or the chiral dissipation induced by the broken  $\mathcal{T}$  symmetry due to the spin-momentum locking in a photonic microstructure. Spin-momentum locking has been the cornerstone for numerous exotic fundamental physics such as photonic Hall effect [77]. In combination with chiral light-matter interaction, it has also become a working horse for constructing chiral quantum optical systems and realizing optical isolation. It is yet to be explored for nonreciprocal phase transition. In many applications, little attention is paid to chiral dissipation. Here, nonreciprocal quantum effect is unveiled by exploring spin-momentum locking and the chiral dissipation. The discovered nonreciprocal photon blockade without using a spinning part may pave the way for unconventional quantum information processing in an integrated platform.

This work was supported by National Key R&D Program of China (Grant No. 2019YFA0308700), Innovation Program for Quantum Science and Technology (Grant No. 2021ZD0301400), the National Natural Science Foundation of China (Grants No. 11890704, No. 92365107, and No. 12305020), the Program for Innovative Talents and Teams in Jiangsu (Grant No. JSSCTD202138), the Shccig-Qinling Program, the China Postdoctoral Science Foundation (Grant No. 2023M731613), and the Jiangsu Funding Program for Excellent Postdoctoral Talent (Grant No. 2023ZB708).



- (2002).
- [2] G. Chapline and M. Nauenberg, Phase transition from baryon to quark matter, *Nature (London)* **264**, 235 (1976).
  - [3] T. W. B. Kibble, Some implications of a cosmological phase transition, *Phys. Rep.* **67**, 183 (1980).
  - [4] Y. K. Wang and F. T. Hioe, Phase transition in the Dicke model of superradiance, *Phys. Rev. A* **7**, 831 (1973).
  - [5] K. Baumann, C. Guerlin, F. Brennecke, and T. Esslinger, Dicke quantum phase transition with a superfluid gas in an optical cavity, *Nature (London)* **464**, 1301 (2010).
  - [6] S. V. Kravchenko, W. E. Mason, G. E. Bowker, J. E. Furneaux, V. M. Pudalov, and M. D'Iorio, Scaling of an anomalous metal-insulator transition in a two-dimensional system in silicon at  $B=0$ , *Phys. Rev. B* **51**, 7038 (1995).
  - [7] D. Bitko, T. F. Rosenbaum, and G. Aeppli, Quantum critical behavior for a model magnet, *Phys. Rev. Lett.* **77**, 940 (1996).
  - [8] S. Sachdev, Quantum criticality: Competing ground states in low dimensions, *Science* **288**, 475 (2000).
  - [9] X.-Y. Luo, Y.-Q. Zou, L.-N. Wu, Q. Liu, M.-F. Han, M. K. Tey, and L. You, Deterministic entanglement generation from driving through quantum phase transitions, *Science* **355**, 620 (2017).
  - [10] S. L. Sondhi, S. M. Girvin, J. P. Carini, and D. Shahar, Continuous quantum phase transitions, *Rev. Mod. Phys.* **69**, 315 (1997).
  - [11] S. Sachdev, Quantum phase transitions, *Phys. World* **12**, 33 (1999).
  - [12] M. Vojta, Quantum phase transitions, *Rep. Prog. Phys.* **66**, 2069 (2003).
  - [13] J. Orenstein and A. J. Millis, Advances in the physics of high-temperature superconductivity, *Science* **288**, 468 (2000).
  - [14] A. D. Greentree, C. Tahan, J. H. Cole, and L. C. L. Hollenberg, Quantum phase transitions of light, *Nat. Phys.* **2**, 856 (2006).
  - [15] N. Mann, M. R. Bakhtiari, A. Pelster, and M. Thorwart, Nonequilibrium quantum phase transition in a hybrid atom-optomechanical system, *Phys. Rev. Lett.* **120**, 063605 (2018).
  - [16] B. Wang, F. Nori, and Z.-L. Xiang, Quantum phase transitions in optomechanical systems, *Phys. Rev. Lett.* **132**, 053601 (2024).
  - [17] C. M. Bender, Making sense of non-Hermitian hamiltonians, *Rep. Prog. Phys.* **70**, 947 (2007).
  - [18] P. Cejnar, S. Heinze, and M. Macek, Coulomb analogy for non-Hermitian degeneracies near quantum phase transitions, *Phys. Rev. Lett.* **99**, 100601 (2007).
  - [19] T. E. Lee, F. Reiter, and N. Moiseyev, Entanglement and spin squeezing in non-Hermitian phase transitions, *Phys. Rev. Lett.* **113**, 250401 (2014).
  - [20] L. Zhou, Q.-h. Wang, H. Wang, and J. Gong, Dynamical quantum phase transitions in non-Hermitian lattices, *Phys. Rev. A* **98**, 022129 (2018).
  - [21] S. Longhi, Topological phase transition in non-Hermitian quasicrystals, *Phys. Rev. Lett.* **122**, 237601 (2019).
  - [22] T. Liu, Y.-R. Zhang, Q. Ai, Z. Gong, K. Kawabata, M. Ueda, and F. Nori, Second-order topological phases in non-Hermitian systems, *Phys. Rev. Lett.* **122**, 076801 (2019).
  - [23] N. Matsumoto, K. Kawabata, Y. Ashida, S. Furukawa, and M. Ueda, Continuous phase transition without gap closing in non-Hermitian quantum many-body systems, *Phys. Rev. Lett.* **125**, 260601 (2020).
  - [24] T. Dai, Y. Ao, J. Mao, Y. Yang, Y. Zheng, C. Zhai, Y. Li, J. Yuan, B. Tang, Z. Li, J. Luo, W. Wang, X. Hu, Q. Gong, and J. Wang, Non-Hermitian topological phase transitions controlled by nonlinearity, *Nat. Phys.* **20**, 101 (2024).
  - [25] P. Peng, W. Cao, C. Shen, W. Qu, J. Wen, L. Jiang, and Y. Xiao, Anti-parity-time symmetry with flying atoms, *Nat. Phys.* **12**, 1139 (2016).
  - [26] C. Liang, Y. Tang, A.-N. Xu, and Y.-C. Liu, Observation of exceptional points in thermal atomic ensembles, *Phys. Rev. Lett.* **130**, 263601 (2023).
  - [27] Y. Wu, W. Liu, J. Geng, X. Song, X. Ye, C.-K. Duan, X. Rong, and J. Du, Observation of parity-time symmetry breaking in a single-spin system, *Science* **364**, 878 (2019).
  - [28] W. Ning, R.-H. Zheng, J.-H. Lü, F. Wu, Z.-B. Yang, and S.-B. Zheng, Experimental observation of spontaneous symmetry breaking in a quantum phase transition, *Sci. China Phys. Mech. Astron.* **67**, 220312 (2024).
  - [29] Z. Yu and S. Fan, Complete optical isolation created by indirect interband photonic transitions, *Nat. Photonics* **3**, 91 (2009).
  - [30] G. T. Reed, G. Mashanovich, F. Y. Gardes, and D. J. Thomson, Silicon optical modulators, *Nat. Photonics* **4**, 518 (2010).
  - [31] H. Lira, Z. Yu, S. Fan, and M. Lipson, Electrically driven nonreciprocity induced by interband photonic transition on a silicon chip, *Phys. Rev. Lett.* **109**, 033901 (2012).
  - [32] N. A. Estep, D. L. Sounas, J. Soric, and A. Alù, Magnetic-free non-reciprocity and isolation based on parametrically modulated coupled-resonator loops, *Nat. Phys.* **10**, 923 (2014).
  - [33] K. Xia, G. Lu, G. Lin, Y. Cheng, Y. Niu, S. Gong, and J. Twamley, Reversible nonmagnetic single-photon isolation using unbalanced quantum coupling, *Phys. Rev. A* **90**, 043802 (2014).
  - [34] C. Sayrin, C. Junge, R. Mitsch, B. Albrecht, D. O'Shea, P. Schneeweiss, J. Volz, and A. Rauschenbeutel, Nanophotonic optical isolator controlled by the internal state of cold atoms, *Phys. Rev. X* **5**, 041036 (2015).
  - [35] M. Scheucher, A. Hilico, E. Will, J. Volz, and A. Rauschenbeutel, Quantum optical circulator controlled by a single chirally coupled atom, *Science* **354**, 1577 (2016).
  - [36] F. Ruesink, M.-A. Miri, A. Alù, and E. Verhagen, Nonreciprocity and magnetic-free isolation based on optomechanical interactions, *Nat. Commun.* **7**, 13662 (2016).
  - [37] S. Zhang, Y. Hu, G. Lin, Y. Niu, K. Xia, J. Gong, and S. Gong, Thermal-motion-induced non-reciprocal quantum optical system, *Nat. Photonics* **12**, 744 (2018).
  - [38] K. Xia, F. Nori, and M. Xiao, Cavity-free optical isolators and circulators using a chiral cross-Kerr nonlinearity, *Phys. Rev. Lett.* **121**, 203602 (2018).
  - [39] R. Huang, A. Miranowicz, J.-Q. Liao, F. Nori, and H. Jing, Nonreciprocal photon blockade, *Phys. Rev. Lett.* **121**, 153601 (2018).
  - [40] P. Yang, X. Xia, H. He, S. Li, X. Han, P. Zhang, G. Li, P. Zhang, J. Xu, Y. Yang, and T. Zhang, Realization of nonlinear optical nonreciprocity on a few-photon level based on atoms strongly coupled to an asymmetric cavity, *Phys. Rev. Lett.* **123**, 233604 (2019).
  - [41] M.-X. Dong, K.-Y. Xia, W.-H. Zhang, Y.-C. Yu, Y.-H. Ye, E.-Z. Li, L. Zeng, D.-S. Ding, B.-S. Shi, G.-C. Guo, and F. Nori, All-optical reversible single-photon isolation at room temperature, *Sci. Adv.* **7**, eabe8924 (2021).
  - [42] X.-X. Hu, Z.-B. Wang, P. Zhang, G.-J. Chen, Y.-L. Zhang, G. Li, X.-B. Zou, T. Zhang, H. X. Tang, C.-H. Dong, G.-C. Guo, and C.-L. Zou, Noiseless photonic non-reciprocity via optically-induced magnetization, *Nat. Commun.* **12**, 2389 (2021).
  - [43] J.-S. Tang, W. Nie, L. Tang, M. Chen, X. Su, Y. Lu, F. Nori, and K. Xia, Nonreciprocal single-photon band structure, *Phys. Rev. Lett.* **128**, 203602 (2022).
  - [44] L. Tang, J. Tang, M. Chen, F. Nori, M. Xiao, and K. Xia, Quantum squeezing induced optical nonreciprocity, *Phys. Rev. Lett.* **128**, 083604 (2022).

- [45] R.-K. Pan, L. Tang, K. Xia, and F. Nori, Dynamic nonreciprocity with a Kerr nonlinear resonator, *Chin. Phys. Lett.* **39**, 124201 (2022).
- [46] R. Fleury, D. Sounas, and A. Alù, An invisible acoustic sensor based on parity-time symmetry, *Nat. Commun.* **6**, 5905 (2015).
- [47] H.-K. Lau and A. A. Clerk, Fundamental limits and non-reciprocal approaches in non-Hermitian quantum sensing, *Nat. Commun.* **9**, 4320 (2018).
- [48] B. Li, R. Huang, X. Xu, A. Miranowicz, and H. Jing, Nonreciprocal unconventional photon blockade in a spinning optomechanical system, *Photon. Res.* **7**, 630 (2019).
- [49] A. McDonald and A. A. Clerk, Exponentially-enhanced quantum sensing with non-Hermitian lattice dynamics, *Nat. Commun.* **11**, 5382 (2020).
- [50] Y.-F. Jiao, S.-D. Zhang, Y.-L. Zhang, A. Miranowicz, L.-M. Kuang, and H. Jing, Nonreciprocal optomechanical entanglement against backscattering losses, *Phys. Rev. Lett.* **125**, 143605 (2020).
- [51] L. Bao, B. Qi, D. Dong, and F. Nori, Fundamental limits for reciprocal and nonreciprocal non-Hermitian quantum sensing, *Phys. Rev. A* **103**, 042418 (2021).
- [52] A. Hashemi, K. Busch, D. N. Christodoulides, S. K. Ozdemir, and R. El-Ganainy, Linear response theory of open systems with exceptional points, *Nat. Commun.* **13**, 3281 (2022).
- [53] W. Ding, X. Wang, and S. Chen, Fundamental sensitivity limits for non-Hermitian quantum sensors, *Phys. Rev. Lett.* **131**, 160801 (2023).
- [54] W. Mao, Z. Fu, Y. Li, F. Li, and L. Yang, Exceptional-point-enhanced phase sensing, *Sci. Adv.* **10**, ead15037 (2024).
- [55] J. Veenstra, O. Gamayun, X. Guo, A. Sarvi, C. V. Meinersen, and C. Coullais, Non-reciprocal topological solitons in active metamaterials, *Nature (London)* **627**, 528 (2024).
- [56] N. P. Kryuchkov, A. V. Ivlev, and S. O. Yurchenko, Dissipative phase transitions in systems with nonreciprocal effective interactions, *Soft Matter* **14**, 9720 (2018).
- [57] M. Fruchart, R. Hanai, P. B. Littlewood, and V. Vitelli, Non-reciprocal phase transitions, *Nature (London)* **592**, 363 (2021).
- [58] Z. Zhang, P. Delplace, and R. Fleury, Superior robustness of anomalous non-reciprocal topological edge states, *Nature (London)* **598**, 293 (2021).
- [59] J. P. Banerjee, R. Mandal, D. S. Banerjee, S. Thutupalli, and M. Rao, Unjamming and emergent nonreciprocity in active ploughing through a compressible viscoelastic fluid, *Nat. Commun.* **13**, 4533 (2022).
- [60] E. I. R. Chiacchio, A. Nunnenkamp, and M. Brunelli, Nonreciprocal Dicke model, *Phys. Rev. Lett.* **131**, 113602 (2023).
- [61] A. Dinelli, J. O'Byrne, A. Curatolo, Y. Zhao, P. Sollich, and J. Tailleur, Non-reciprocity across scales in active mixtures, *Nat. Commun.* **14**, 7035 (2023).
- [62] H. Alston, L. Cocconi, and T. Bertrand, Irreversibility across a nonreciprocal  $\mathcal{PT}$ -symmetry-breaking phase transition, *Phys. Rev. Lett.* **131**, 258301 (2023).
- [63] S. Verma and M. J. Park, Topological phase transitions of generalized Brillouin zone, *Commun. Phys.* **7**, 21 (2024).
- [64] C. Tang, H. Yang, L. Song, X. Yao, P. Yan, and Y. Cao, Competition of non-Hermitian skin effect and topological localization of corner states observed in circuits, *Phys. Rev. B* **108**, 035410 (2023).
- [65] A. Wang, Z. Meng, and C. Q. Chen, Non-Hermitian topology in static mechanical metamaterials, *Sci. Adv.* **9**, eadf7299 (2023).
- [66] J. Park, H. Cho, S. Lee, K. Lee, K. Lee, H. C. Park, J.-W. Ryu, N. Park, S. Jeon, and B. Min, Revealing non-Hermitian band structure of photonic Floquet media, *Sci. Adv.* **8**, eabo6220 (2022).
- [67] H. Wu, Y. Ruan, Z. Li, M.-X. Dong, M. Cai, J. Tang, L. Tang, H. Zhang, M. Xiao, and K. Xia, Fundamental distinction of electromagnetically induced transparency and Autler-Townes splitting in breaking the time-reversal symmetry, *Laser Photonics Rev.* **16**, 2100708 (2022).
- [68] P. Lodahl, S. Mahmoodian, S. Stobbe, A. Rauschenbeutel, P. Schneeweiss, J. Volz, H. Pichler, and P. Zoller, Chiral quantum optics, *Nature (London)* **541**, 473 (2017).
- [69] L. Tang, J. Tang, W. Zhang, G. Lu, H. Zhang, Y. Zhang, K. Xia, and M. Xiao, On-chip chiral single-photon interface: Isolation and unidirectional emission, *Phys. Rev. A* **99**, 043833 (2019).
- [70] T. V. Mechelen and Z. Jacob, Universal spin-momentum locking of evanescent waves, *Optica* **3**, 118 (2016).
- [71] Y. Choi, S. Kang, S. Lim, W. Kim, J.-R. Kim, J.-H. Lee, and K. An, Quasieigenstate coalescence in an atom-cavity quantum composite, *Phys. Rev. Lett.* **104**, 153601 (2010).
- [72] D. A. Steck, *Quantum and Atom Optics* (2007).
- [73] J.-S. Tang, L. Tang, and K. Xia, Three methods for the single-photon transport in a chiral cavity quantum electrodynamics system, *Chin. Opt. Lett.* **20**, 062701 (2022).
- [74] R. Kononchuk, J. Cai, F. Ellis, R. Thevamaran, and T. Kottos, Exceptional-point-based accelerometers with enhanced signal-to-noise ratio, *Nature (London)* **607**, 697 (2022).
- [75] K. Takata, K. Nozaki, E. Kuramochi, S. Matsuo, K. Takeda, T. Fujii, S. Kita, A. Shinya, and M. Notomi, Observing exceptional point degeneracy of radiation with electrically pumped photonic crystal coupled-nanocavity lasers, *Optica* **8**, 184 (2021).
- [76] B. Dayan, A. S. Parkins, T. Aoki, E. P. Ostby, K. J. Vahala, and H. J. Kimble, A photon turnstile dynamically regulated by one atom, *Science* **319**, 1062 (2008).
- [77] K. Y. Bliokh, D. Smirnova, and F. Nori, Quantum spin Hall effect of light, *Science* **348**, 1448 (2015).